TIMELESS promotes the proliferation and migration of lung adenocarcinoma cells by activating EGFR through AMPK and SPHK1 regulation

Houqing Yin
Peking University Health Science Center
Zequn Wang (2111210019@stu.pku.edu.cn)
Peking University Health Science Center
Dan Wang
Peking University Health Science Center
Muhadaisi Nuer
Xinjiang Medical University
Mengyuan Han
Xinjiang Medical University
Peng Ren
Peking University Third Hospital
Shanwu Ma
Peking University Third Hospital
Chutong Lin
Peking University Third Hospital
Jingjing Chen
Changzhi Medical College
Haocheng Xian
Peking University Health Science Center
Dongmei Ai
University of Science and Technology Beijing
Xuejun Li
Peking University Health Science Center
Shaohua Ma
Peking University Third Hospital
Zhiqiang Lin
Peking University Health Science Center
Yan Pan
Peking University Health Science Center

Research Article

Keywords: Lung adenocarcinoma, TIMELESS, epidermal growth factor receptor, sphingosine kinase 1, AMP-activated protein kinase

Posted Date: November 1st, 2022

DOI: https://doi.org/10.21203/rs.3.rs-2157503/v1

TIMELESS promotes the proliferation and migration of lung adenocarcinoma cells by activating EGFR through AMPK and SPHK1 regulation

Houqing Yin[a], Zequn Wang[a], Dan Wang[a], Muhadaisi Nuer[e], Mengyuan Han[e], Peng Ren[d], Shanwu Ma[d], Chutong Lin[d], Jingjing Chen[f], Haocheng Xian[a], Dongmei Ai[g], Xuejun Li[a,b], Shaohua Ma[d]*, Zhiqiang Lin[c]*, Yan Pan[a,b]*

[a] Department of Pharmacology, School of Basic Medical Sciences, Health Science Center, Peking University, Beijing 100191, China
[b] Beijing Key Laboratory of Tumor Systems Biology, Peking University, Beijing 100191, China
[c] Institute of Systems Biomedicine, Beijing Key Laboratory of Tumor Systems Biology, School of Basic Medical Sciences, Peking University Health Science Center, Beijing 100191, China
[d] Peking University Third Hospital Thoracic Surgery Department
[e] Department of Pharmacology, Xinjiang Medical University, Urumqi, Xinjiang 830011, China
[f] Department of Pharmacology, Changzhi Medical college, Changzhi City, Shanxi Province 046000, China
[g] School of Mathematics and Physics, University of Science and Technology Beijing, Beijing, 100083, China,

*Correspondence authors:
doctor_msh@bjmu.edu.cn
zhiqiang_lin@bjmu.edu.cn
pannay26@bjmu.edu.cn

ABSTRACT

Background: Lung adenocarcinoma (LUAD) has high morbidity and is prone to recurrence. TIMELESS (TIM), which regulates circadian rhythms in Drosophila, is highly expressed in various tumors.

Methods：We used tumor samples from patients with lung carcinoma and LUAD patient data from public databases to confirm the relationship of TIM expression with lung cancer. We used NSCLC cell lines and siRNA to knock down TIM expression, and further analyzed cell proliferation, migration and colony formation. By using western blot and qPCR, we detected the influence of TIM on EGFR, Sphk1 and AMPK. With proteomics analysis, we comprehensively inspected the different changed proteins influenced by TIM and did global bioinformatic analysis.

Results: In this study, we found that TIM expression was elevated in LUAD and that this high expression was positively correlated with more advanced tumor pathological stages and shorter overall and disease-free survival. Moreover, gefitinib efficacy in patients with LUAD could be influenced by TIM expression, and the antitumor effect of gefitinib was significantly improved with TIM knockdown. TIM knockdown inhibited epidermal growth factor receptor (EGFR) activation and phosphorylation of its downstream AKT/mTOR and ERK1/2 pathways. We also clarified that TIM regulated the activation of sphingosine kinase 1 (SPHK1) in LUAD cells, while SPHK1 knockdown inhibited EGFR activation. Quantitative proteomics techniques combined with bioinformatics analysis were adopted to clarify the global molecular mechanisms regulated by TIM in LUAD. The results of proteomics suggested that mitochondrial translation elongation and termination were altered, which were closely related to the process of mitochondrial oxidative phosphorylation. Knockdown of TIM reduced the ATP content and promoted AMP-activated protein kinase (AMPK) activation.

Conclusions: Our study revealed that TIM could regulate EGFR activation through AMPK and SPHK1, as well as influence mitochondrial function and alter the ATP level; thus, TIM is a key factor in LUAD.

Keywords: Lung adenocarcinoma, TIMELESS, epidermal growth factor receptor, sphingosine kinase 1, AMP-activated protein kinase

Background

Lung cancer is a malignant cancer with high incidence. Indeed, lung cancer is the leading cause of cancer deaths, with non-small-cell lung cancer (NSCLC) accounting for 85% of lung cancers. Lung adenocarcinoma (LUAD) and lung squamous carcinoma (LUSC) are the two most important types of NSCLC, with LUAD accounting for 85% of NSCLC cases[1-3]. The current treatment for LUAD includes surgical resection, radiotherapy, chemotherapy, targeted therapy, and immunotherapy[4]. Despite great progress in treatment, the 5-year survival rate of patients with LUAD remains poor, with tumor recurrence and drug resistance remaining common and posing fatal threats to patients[5-8]. Therefore, it is still necessary to clarify the mechanism of occurrence and development of lung cancer and to find novel curative strategies.

Circadian clock genes have been shown to play an important role in tumorigenesis. Indeed, circadian clock genes are closely associated with multiple functional features of tumors, including cell proliferation, apoptosis, angiogenesis, immune surveillance, and tumor cell metabolism[9]. For example, in colorectal cancer, overexpression of the circadian clock gene BMAL1 could inhibit tumor cell proliferation and increase tumor cell sensitivity to oxaliplatin in vivo[10]. Moreover, the circadian clock gene CLOCK was found to drive immunosuppression in glioblastoma[11]. In oral squamous cell carcinoma, overexpression of the circadian clock gene PER2 promotes tumor cell autophagy and apoptosis and inhibited tumor cell proliferation[12]. TIMELESS (TIM), as another circadian clock gene, has also been found to play an important role in tumors by regulating DNA replication, DNA damage repair, and cell proliferation[13-16]. Indeed, TIM is highly expressed in several types of cancers, including lung, breast, liver, colorectal, and cervical cancers[17-21]. Our previous research also found that TIM was highly expressed in lung cancer, in which high expression of TIM was closely related to the shortened overall and progression-free survival of patients[22]. However, the role and specific mechanisms of TIM in tumorigenesis and development, especially in LUAD, remain unclear. Therefore, in the present study, we used siRNA interference on LUAD cell lines and lung cancer tissues of patients with LUAD to detect the influence of TIM on cell proliferation and migration. Additionally, we further examined the regulation of TIM on EGFR activation, an important oncogene in LUAD. Finally, we applied comprehensive proteomics and combined this with biological information analysis to clarify the global regulation of TIM and establish the key mechanisms of TIM in LUAD.

Materials and Methods

Tumor samples from patients with lung carcinoma

Lung carcinoma tissues and tissues adjacent to cancer were collected from patients diagnosed with LUAD during surgery. Samples were not collected if the patients met any of the following exclusion criteria: treated with chemotherapeutic drugs or radiation therapy; presence of other malignant tumors; presence of other immune system diseases; or presence of infectious diseases of the blood system. All patients signed the informed consent form. A lung cancer area of approximately 5 mm × 5 mm was used for analysis. All of the experiments were conducted following approval from the

Ethics Committees of Peking University. Written informed consent was obtained from all patients prior to tissue sample collection.

LUAD patient data in public databases

The data of LUAD samples were extracted from The Cancer Genome Atlas (TCGA; https://cancergenome.nih.gov) and samples from patients without sufficient data were excluded from subsequent analyses. Data from normal lung tissue samples were also obtained in Genotype-Tissue Expression (GTEx) (https://gtexportal. org/home/datasets).

TNMplot database analysis

RNA-seq data from TCGA and GTEx of 524 tumor tissues and 468 normal lung tissue samples taken from patients with LUAD were downloaded from the TNMplot online analysis platform (https://www.tnmplot.com) for TIM gene-level analysis and were analyzed for significance using the Mann–Whitney test.

UALCAN database analysis

RNA-seq data of 515 tumor tissue samples and 59 normal lung tissue samples taken from patients with LUAD were collected from TCGA database and downloaded from the UALCAN online tool (http://ualcan.path.uab.edu) for *SPHK1* gene-level analysis. Mann–Whitney test was used to determine statistical significance.

HPA database analysis

The Human Protein Atlas (HPA) database (www.proteininatlas.org) provides protein expression profiles and protein localization with immunohistochemical analysis[23]. The protein expression of TIM and SPHK1 in LUAD was analyzed using the HPA database.

Survival rate analysis

The correlation analysis of *TIM* and *SPHK1* gene levels with the overall survival (OS) and disease-free survival (DFS) of patients with LUAD was performed using the GEPIA2 online tool (http://gepia2.cancer-pku.cn/). Log-rank test was used for hypothesis testing, and the grouping threshold was set to "Median." The hazard ratio (HR) with 95% confidence intervals and log-rank *p*-value were calculated.

Prediction of gefitinib efficacy in patients with LUAD

The Genomics of Drug Sensitivity in Cancer database (GDSC, https://www.cancerrxgene.org/)[24] was used to predict the efficacy of gefitinib for each LUAD sample. The prediction process was implemented using the R software package "pRRophetic," where the gefitinib IC50 was estimated using ridge regression. The batch effect of "combat" and the tissue type of "allSoldTumours" were

removed, and the duplicate gene expression was summarized as mean values and analyzed for significance using the Wilcox test.

Cell culture

A549, H1975, and H1299 cells were cultured in DMEM medium (Gibco, NY, USA) containing 10% (v/v) fetal bovine serum (FBS), 100 U/mL penicillin, and 100 mg/mL streptomycin (Biodee, Beijing, China). HCC827 cells were cultured in RPMI-1640 medium (Cytia, Utah, USA) containing 10% (*v/v*) FBS, 100 U/mL penicillin, and 100 μg/mL streptomycin (Biodee, Beijing, China). All cells were cultured at 37°C in a 5% CO_2 incubator (Thermo Fisher, California, USA).

Cell transfection

Cells were inoculated in 6-well cell culture plates with DMEM or RPMI-1640 medium containing 10% (*v/v*) FBS at a density of 7×10^4 cells per well. Prior to transfection, the cell medium was replaced with DMEM or RPMI-1640 medium without FBS, and Lipofectamine^{TM} RNAiMAX and siRNA were diluted with Opti-MEM medium. The transfection solution was mixed at a ratio of 1:1 for 8 h. Subsequently, the transfection medium was replaced with DMEM or RPMI-1640 medium containing 10% (*v/v*) FBS for 24–72 h before conducting subsequent experiments. The siRNA sequences are listed in Table 1.

Cell proliferation

Cells in the logarithmic growth phase were digested with trypsin, adjusted to 5000 cells per well of a 96-well plate, and cultured for 24–72 h. Subsequently, the culture medium in the wells was gently aspirated, and 100 μL of serum-free culture medium containing 10% (v/v) CCK8 was added to each well and allowed to incubate for 3 h. Finally, the absorbance of each well was detected with a microplate reader (Thermo Fisher, California, USA) at 450 nm. Five replicate wells were set per group, and the experiment was repeated at least three times independently.

Cell migration

Cells in the logarithmic growth phase were digested with trypsin and added to the Transwell upper chamber containing DMEM medium supplemented with 1% (v/v) FBS. The Transwell lower chamber contained DMEM medium supplemented with 10% FBS. The cells were cultured for 48 h before the medium in the chamber was discarded. The chambers were washed twice with PBS, and 4% paraformaldehyde was used to fix cells at room temperature for 20 min. Then, the chamber was air-dried and stained with 0.1% crystal violet for 20 min. A cotton swab was used to gently wipe off the cells on the top of the upper chamber that had not crossed into the backside of the chamber. Finally, the cells on the backside of this upper chamber were detected under an Olympus microscope; five fields of view in each well were recorded, and the ImageJ software (Version 1.51) was used to analyze the data.

Western blot

Tumor cell lysates were prepared using RIPA lysate (containing protease inhibitors). The protein concentration was determined by the BCA method. Cell lysates were separated on SDS-PAGE and transferred onto polyvinylidene fluoride (PVDF) membranes. Non-specific binding sites were blotted with 5% milk and specific sites were treated with 5% bovine serum albumin (BSA) (both containing TBST) at room temperature for 1 h. Then, the membranes were incubated at 4°C overnight using the indicated primary antibodies, followed by incubation with secondary antibodies at room temperature for 1 h. The membranes were visualized using the ECL system (Syngene, Cambridge, UK), and ImageJ software (Version 1.51) was used for the densitometric analysis of immunoblot band intensities. The following primary antibodies, diluted in PBS at a ratio of either 1:1000 or 1:2000, were used: TIMELESS Mouse Monoclonal Antibody (Proteintech, Illinois, USA), β-Actin (13E5) Rabbit Monoclonal Antibody (Cell Signaling Technology, Massachusetts, USA), EGFR Mouse Monoclonal Antibody (Proteintech, Illinois, USA), Phospho-EGFR (Y1068), EGFR Rabbit Polyclonal Antibody (Abclonal, Wuhan, China), AKT Rabbit Polyclonal Antibody (Proteintech, Illinois, USA), Phospho-AKT (Ser473) Monoclonal Antibody (Abcam, Cambridge, UK), mTOR Rabbit Monoclonal Antibody (Cell Signaling Technology, Massachusetts, USA), Phospho-mTOR (Ser2448) Rabbit Monoclonal Antibody (Cell Signaling Technology, Massachusetts, USA), SPHK1 Rabbit Polyclonal Antibody (Beyotime, Shanghai, China), STAT3 Rabbit Monoclonal Antibody (Beyotime, Shanghai, China), Phospho-STAT3 (Ser727) Rabbit Monoclonal Antibody (Abclonal, Wuhan, China), ATF3 Rabbit Monoclonal Antibody (Cell Signaling Technology), Phospho-AMPKα (Thr172) Rabbit Monoclonal Antibody (Cell Signaling Technology, Massachusetts, USA), and AMPKα Rabbit Monoclonal Antibody (Cell Signaling Technology, Massachusetts, USA). The secondary antibodies used were HRP conjugate Goat Anti-Mouse IgG (Proteintech, Illinois, USA) and HRP conjugate Goat Anti-Rabbit IgG (Proteintech, Illinois, USA).

RT-qPCR assay

Total RNA was extracted from cells using TRIzol, and the total RNA purity was checked by a UV spectrophotometer. The cDNA was synthesized using the cDNA First Strand Synthesis Kit (Gemma Biology Corporation, Beijing, China). RT-qPCR was performed using the SYBR Green Fast qPCR Mix. GAPDH was used as an internal reference, and the relative expression of target genes was analyzed according to the $2^{-\Delta\Delta Ct}$ method. The primer sequences are listed in Table 2.

Proteomics sample preparation, LC-MS analysis, and protein identification

Cells were lysed with RIPA lysis solution containing protease inhibitors and lysed by ultrasonification three times. The lysis supernatant was collected, and the protein concentration was determined using the BCA method. Protein sample preparation and LC-MS analysis were carried out according to the method of Zhou[25]. Protein identification and label-free quantification were performed using MaxQuant version 1.5.1.6, with the default settings used by Zhou[25].

Functional enrichment analysis

The R package “limma” was used to screen differentially expressed proteins influenced by TIM knockdown. The package version used in this study was 3.18.0. The threshold was defined as

$|\log_2(FC)| > 1$ and adjusted *p-value* < 0.05, and the R package "clusterProfiler" and "pathview" were used to perform the Gene Ontology (GO) and Kyoto Encyclopedia of Genes and Genomes (KEGG) pathway enrichment analyses on differentially expressed proteins. Gene set enrichment analysis (GSEA) software (http://software.broadinstitute.org/gsea/index.jsp) was used, and c6.all.v7.4.symbols.gmt was downloaded from the Molecular Signatures Database (http://www.gseamsigdb.org/gsea/downloads.jsp). Subsets to evaluate related pathways and molecular mechanisms were grouped based on gene expression profiles and phenotypes, with the minimum gene number set to 5, the maximum gene number was set to 5000. A *p-value* < 0.05 and a false discovery rate (FDR) < 0.25 were considered statistically significant.

Detection of intracellular ATP content

The concentration of ATP was measured using the ATP detection assay kit (Beyotime, Shanghai, China), following the luciferin-luciferase method. Briefly, cells were cultured in a 6-well plate before being washed twice with PBS and adding 200 μL of lysis solution. The cells were blown repeatedly to fully lyse, following which, they were centrifuged at 4°C for 5 min at 12000 g, and the supernatant was aspirated carefully for use. The ATP standard solution was diluted into gradients of 0.01, 0.03, 0.1, 0.3, 1, 3, and 10 μmol/L using the ATP assay lysate. The ATP assay reagent was diluted with ATP assay diluent at a ratio of 1:9 to prepare the ATP assay working solution. Subsequently, 100 μL of ATP working solution was added to each well of a 96-well plate and incubated at room temperature for 3–5 min to reduce background ATP. Subsequently, 20 μL of sample or standard solution was added, shaken, and mixed, and after a 3-s interval, the relative light unit (RLU) value was measured by chemiluminescence. The ATP concentration of each sample was calculated according to the RLU value-concentration standard curve of the standard sample.

Statistical analysis

All data were statistically analyzed with GraphPad Prism software (version 8.0), and all data are shown as the mean ± SD. Unpaired two-tailed Student's *t*-test (when variances were consistent) or Welch's corrected t-test (when variances were inconsistent) was used for the analysis of two samples. One-way ANOVA with Dunnett's multiple comparison test was used for the analysis of multiple samples.

Results

TIM is highly expressed in patients with LUAD and correlates with poor patient prognosis

To explore the changes in circadian clock genes in NSCLC, we used RT-qPCR assay to detect the mRNA level of the circadian clock genes *BMAL1*, *CLOCK*, *PER1*, *PER2*, *CRY1*, *CRY2*, *TIM,* and *REV-ERBα* in tumor tissues. The results showed that the *TIM* mRNA level was significantly upregulated ($p < 0.05$) in tumor tissues compared to normal lung tissues (Figure 1A). We then used the R package "ggplot2" to analyze the relationship between the *TIM* mRNA level and the tumor

pathological stage of patients. The results showed that upregulation of the *TIM* mRNA level was associated with advanced pathological stage (Figure 1B).

To further evaluate the changes of TIM in LUAD, we used the TNMplot online tool and found that the TIM level was significantly higher in tumor tissues compared to normal lung tissues ($p < 0.01$) (Figure 1C). We also examined the protein expression level of TIM in NSCLC using the Human Protein Atlas database and observed that TIM was highly expressed in tumor tissues compared to normal lung tissues (Figure 1D).

Using the GEPIA2 online tool, we divided the sample of patients with LUAD into high-TIM expression level and low-TIM expression level and assessed the prognostic value of TIM by univariate Cox regression analysis. The results showed that the TIM level was significantly positively correlated with the OS and DFS of patients with LUAD ($p < 0.01$), that is, the higher the TIM expression level, the shorter the OS and DFS of patients will be (Figure 1E). Then, based on the Genomics of Drug Sensitivity in Cancer database and using the R software package "pRRophetic," we predicted the IC_{50} value of gefitinib in patients with NSCLC with different TIM expression levels. The IC_{50} value of gefitinib will be lower in patients with low TIM expression than in those with high TIM expression. We deduced that these patients with low TIM expression were more sensitive to gefitinib (Figure 1F).

TIM knockdown inhibits the proliferation and migration of LUAD cells and sensitizes the antitumor effect of gefitinib

We also detected the protein expression level of TIM in four LUAD cell lines. TIM expression was slightly higher in A549, H1975, and H1299 cells compared to HCC827 cells (Figure 2A). We confirmed that the TIM mRNA level in H1975 and HCC827 cells was consistent with the protein expression level (Figure 2B). Therefore, we selected H1975 and HCC827 for the later experiments. We further found that the TIM level in H1975 cells showed a dynamic change within 24 h, gradually increasing from 0 h and reaching a peak at 8 h (Figure 2C). The TIM protein levels at 0 h and 8 h were consistent with the TIM mRNA level (Figure 2D). Therefore, we chose 8 h as the detected time point for the subsequent experiments.

We constructed TIM siRNA and confirmed that the third pair of TIM siRNA (siTIM#3) had the best knockdown efficiency, with 53% TIM expression knockdown (Figure 3A). Next, using TIM siRNA, we examined the influence of TIM on the proliferation of H1975 cells. The results showed that TIM knockdown could significantly inhibit cell proliferation ($p < 0.01$) (Figure 3B) and cell migration of H1975 cells ($p < 0.01$, Figure 3C).

TIM knockdown may also increase the effects of gefitinib. In H1975 cells, TIM knockdown combined with 1.0×10^{-5} mol/L gefitinib showed significantly increased inhibitory effects on cell proliferation compared to gefitinib alone ($p < 0.01$, Figure 3D and 3E).

TIM knockdown inhibits activation of EGFR and its downstream signaling pathway

EGFR and its downstream PI3K/AKT/mTOR and RAS/RAF/ERK1/2 pathways are critical for promoting tumor cell growth and inhibiting apoptosis in LUAD[26]. EGFR is also the target of gefitinib[27-28]; therefore, we sought to determine whether TIM knockdown could influence the expression and activation of EGFR. Our results showed that TIM knockdown resulted in a significant inhibition of EGFR activation, had no significant impact on EGFR expression, and inhibited the activation of AKT and mTOR ($p < 0.0$, Figure 4).

We then detected the mRNA level of two EGFR ligands, epidermal growth factor (*EGF*) and amphiregulin (*AREG*). However, the mRNA level of EGF and AREG was unaffected by TIM knockdown (Figure 4E).

Oncogenes such as *BCRP*, *MYBL2*, *CCND1*, *c-MYC*, *AURKA*, *PTGS2*, and *TYMS* can be regulated by EGFR in LUAD and can promote tumor development[29-30]. In H1975 cells, TIM knockdown significantly downregulated the level of *c-MYC* and *AURKA* ($p < 0.05$, Figure 5A and 5B).

TIM promotes EGFR activation by regulating SPHK1

TIM is known to promote the synthesis of sphingosine 1-phosphate (S1P) in breast cancer[31]. SPHK1 is the key intracellular kinase that catalyzes the production of S1P from sphingosine[32]; therefore, we investigated whether TIM affects SPHK1. The results showed that TIM knockdown significantly decreased SPHK1 expression ($p < 0.05$), STAT3 activation ($p < 0.05$), and ATF3 expression ($p < 0.01$) both in H1975 cells (Figure 6A) and HCC827 cells (Figure 6B). Moreover, following knockdown of SPHK1 in H1975 cells, EGFR activation was inhibited and the activation of AKT and mTOR was reduced in both H1975 and HCC827 cells (Figure 6C).

Furthermore, *SPHK1* mRNA levels were upregulated in the tumor tissues of patients with LUAD patients when compared to normal lung tissues (Supplementary Figure 1A). The data from UALCAN and the HPA database both proved that SPHK1 is significantly elevated in tumor tissues ($p < 0.01$, Supplementary Figure 1B and 1C). Further analysis revealed that the expression level of SPHK1 in patients with LUAD was significantly negatively correlated with the OS ($p < 0.05$); that is, the higher the SPHK1 expression level, the shorter the OS of the patient (Supplementary Figure 1D).

Comprehensive quantitative proteomics combined with bioinformatics analysis implies a key role of TIM in LUAD

We next performed the quantitative proteomics to investigate the global influences of TIM on LUAD. The differentially expressed proteins were screened according to $|\log_2(FC)| > 1$, adjusted *p-value* < 0.05. A total of 98 differentially expressed proteins were obtained, among which, 33 proteins were significantly upregulated and 65 proteins were significantly downregulated after TIM knockdown (Figure 7A). GO enrichment analysis showed that differentially expressed proteins mainly mediated mitochondrial translational elongation and mitochondrial translational termination

at the biological process (Figure 7B), mainly mediated ribosomal subunit and ribosome at the cellular component (Figure 7C), and were mainly enriched in catalytic activity acting on RNA and cadherin binding at the molecular function (Figure 7D). KEGG pathway enrichment analysis showed that differentially expressed proteins mainly regulate ribosome biogenesis in eukaryotes and amino sugar and nucleotide sugar metabolism (Figure 7E). We further found that among the top 10 significantly enriched GO biological processes, *MRPS5*, *MRPL3*, *MRPL50*, *MRPL44*, *GADD45GIP1*, *MRPL43*, *TEX10*, *UTP14A*, *BYSL*, *NOL6*, *DDX52*, *RPP40*, *RPL7L1*, and *NOB1* were the most involved genes. Among them, *MRPS5*, *MRPL3*, *MRPL50*, *MRPL44*, *GADD45GIP1*, and *MRPL43* were involved in mitochondrial translation elongation, mitochondrial translation termination, translation termination, and cellular protein complex disassembly; *TEX10*, *UTP14A*, *BYSL*, *NOL6*, *DDX52*, *RPP40*, *NOB1*, *RPL7L1*, and *NOB1* were involved in the regulation of mitochondrial translation elongation; and *DDX52, RPP40*, *RPL7L1*, and *NOB1* were involved in the regulation of rRNA processing, ribosome biogenesis, and rRNA metabolic process (Figure 7F). Oncogenic signature-based GSEA showed that the genes influenced by TIM knockdown were enriched in the EGFR_UP. V1_DN and MYC_UP. V1_UP gene sets (Figure 7G).

Effects of TIM on cellular ATP content and AMPK activation

The proteomic results suggest that TIM affects mitochondrial translation elongation and termination, which could influence the synthesis of oxidative phosphorylation complex proteins[33-34]. Therefore, we next analyzed the ATP content in H1975 cells. The results showed that TIM knockdown greatly reduced the intracellular ATP content in H1975 cells (Figure 8A). AMPK, an intracellular energy sensor, was highly activated by TIM knockdown in H1975 cells (Figure 8B). Specifically, we treated H1975 cells with 10 mmol/L of metformin for 8 h and found a significant increase in AMPK activation ($p < 0.01$), as well as a significant inhibition of SPHK1 expression, STAT3 activation, and ATF3 expression ($p < 0.01$) (Figure 8C).

Discussion

The role of TIM in the growth, metastasis, and chemoresistance of various tumors has been reported. Additionally, the role and mechanism of TIM in LUAD have been studied recently, although its detailed function in LUAD has not yet been fully elucidated. In the present study, we adopted clinical LUAD patient lung carcinoma tissue samples and human LUAD cell lines to confirm the correlation of TIM with tumor occurrence and development, before clarifying its ability to regulate EGFR activation through SPHK1. Moreover, using proteomics analysis, we discovered the influence of TIM on mitochondrial functions, confirming the change in mitochondrial ATP and ROS level. Simultaneously, we proved that the regulatory effect of TIM on SPHK1/EGFR is adjusted by AMPK activation (Figure 9, created with BioRender.com).

High expression of TIM in LUAD is associated with poor OS and DFS of patients, and our results are consistent with those of other reports. Zhang Y et al. reported that the TIM expression level was significantly elevated in patients with NSCLC and that high TIM expression was closely related to the tumor size, differentiation, TNM stage, and lymph node metastasis[35]. Yoshida K et al.

also found that an elevated TIM expression level was associated with significantly shorter OS in patients with NSCLC, and the 5-year survival rates of patients with high and low TIM expression levels were 50.2% and 79.2%, respectively[18].

Studies on lung carcinoma cells have shown that TIMs can promote cell proliferation and inhibit apoptosis[18]. In our study involving LUAD cell lines, TIM was found to promote cell proliferation and migration. Moreover, TIM affected the efficacy of gefitinib on tumor cell proliferation, suggesting that patients with LUAD with low TIM expression might be more sensitive to gefitinib. Indeed, the IC_{50} of gefitinib in such patients was lower than that in patients with high TIM expression.

The transmembrane tyrosine kinase receptor protein EGFR is crucial in the development of LUAD. The ligands of EGFR bind to its extracellular domain and promote the phosphorylation of the intracellular tyrosine kinase region, which activates downstream pathways such as RAS/MAPK and PI3K/AKT/mTOR[26, 36-38]. Gefitinib, an EGFR tyrosine kinase inhibitor, binds competitively to the highly conserved ATP site of the EGFR intracellular tyrosine kinase region and inhibits EGFR phosphorylation and activation[27-28]. Our results showed that TIM knockdown significantly inhibited EGFR activation in LUAD cells but had no influence on the mRNA level of EGF and AREG, two EGFR ligands. As previous studies on A549 and GLC82 tumor cells have revealed that EGFR can upregulate the mRNA level of oncogenes *CCND1*, *PTGS2*, and *c-MYC*[30], we next detected the levels of these oncogenes. Our results showed that TIM knockdown significantly downregulated *c-MYC* and *AURKA*. Some studies have proven that EGFR can transfer from the membrane to the nucleus, where it regulates the transcription of *c-MYC* and *AURKA* and promotes tumor growth[29-30]. We deduced that this regulation may be related to nuclear EGFR.

Overexpression of SPHK1 has been shown to promote EGFR activation in EC9704-P6 esophageal cancer cells, whereas knockdown of SPHK1 reduced EGFR activation[39]. A previous study on colorectal cancer showed that treatment with the SPHK1 inhibitor FTY720 inhibited activation of EGFR and downstream AKT in a tumor-bearing mouse model[40]. Moreover, in MDA-MB-231 and MDA-MB-436 breast cancer cells, both SPHK1 knockdown and the SPHK1 inhibitor SKi-II blocked the activation of EGFR and AKT[41]. It has also been reported that S1P, the product of SPHK1, can promote EGFR activation[42-44]. Additionally, some researchers have found that TIM knockdown can downregulate the level of S1P in breast cancer cells[31]. Therefore, we speculate that the regulation of EGFR by TIM was related to SPHK1/S1P signaling. Our results proved that TIM knockdown significantly inhibited the expression of SPHK1 and activation of STAT3. Furthermore, we found that SPHK1 was highly expressed in LUAD, and knockdown of SPHK1 inhibited EGFR phosphorylation and AKT/mTOR activation; this implies that the regulation of EGFR by TIM occurs via SPHK1/STAT3.

SPHK1 was found to promote the proliferation and migration of NSCLC cells through activation of STAT3[45]. SPHK1 could also induce STAT3 activation to promote the invasion of head and neck squamous cell carcinoma[46]. The SPHK1/STAT3 pathway has also been found to mediate the invasion and metastasis of colorectal cancer and promote cisplatin resistance in bladder cancer cells[47-48].

TIM knockdown has been shown to inhibit the expression of ATF3, a key factor in controlling the expression of cell cycle regulatory genes, tumor suppressor genes, DNA repair genes, and apoptosis genes. Increasing evidence suggests that ATF3 also plays a crucial role in tumor development[49]. Indeed, in lung cancer, high expression of ATF3 is significantly correlated with advanced tumor grade, lymph node metastasis, and shortened OS, while ATF3 knockdown can significantly inhibit the proliferation and migration of lung cancer cells[50]. Moreover, in skin cancer, ATF3 was found to promote tumor cell proliferation by activating STAT3, enhancing the development of skin keratinocyte tumors[51].

Proteomic techniques have the advantage of elucidating the molecular characteristics of tumors to explore the underlying pathogenesis and to develop new tumor therapeutic targets. Therefore, we next performed proteomic analysis of LUAD cells with TIM knockdown to further explore the comprehensive molecular mechanism underlying the effects of TIM on the occurrence and development of LUAD. The results suggested that TIM may have regulatory effects on mitochondrial translation and ribosomal biogenesis functions in LUAD cells. The mitochondrial translation process affects the synthesis of the basic protein subunits that constitute the mitochondrial respiratory chain complex[33-34] and accordingly ATP production. It has also been reported that TIM knockdown significantly inhibits mitochondrial respiration in breast cancer cells[31]. Accordingly, we believe that TIM could affect the mitochondrial oxidative phosphorylation process and thus the ATP content in LUAD cells.

AMPK, an evolutionarily conserved serine/threonine kinase that acts as an intracellular energy sensor, is activated when the intracellular ATP level declines[88]. AMPK activation promotes catabolic pathways and inhibits ATP-consuming anabolic pathways to restore energy homeostasis[87, 88]. We observed a change in AMPK with the decrease in ATP in LUAD cells. Moreover, knockdown of TIM in LUAD cells resulted in significant activation of AMPK.

Furthermore, in ovarian cancer, metformin, which activates AMPK, was found to inhibit hypoxia-induced SPHK1 expression, as well as the enhanced cell proliferation caused by SPHK1 overexpression[52]. AMPK activation can also inhibit S1P-promoted airway smooth muscle cell proliferation[53]. In LUAD cells, we found that metformin could inhibit SPHK1 expression and activate AMPK phosphorylation. Taken together, we deduced that TIM plays a role in LUAD by influencing AMPK/SPHK1/EGFR molecules.

Conclusion

TIM promotes cell proliferation and migration by regulating EGFR activation via AMPK and SPHK1. TIM may have global effects on mitochondrial translation and ribosomal biogenesis, as well as on mitochondrial ATP content and AMPK activation. Therefore, TIM is important in the development of LUAD and represents a potential therapy target in the future.

Abbreviations

LUAD	Lung adenocarcinoma
TIM	TIMELESS
EGFR	Epidermal growth factor receptor
SPHK1	Sphingosine kinase 1
AMPK	AMP-activated protein kinase
NSCLC	Non-small-cell lung cancer
LUSC	Lung squamous carcinoma
TCGA	The Cancer Genome Atlas
GTEx	Genotype-Tissue Expression
HPA	The Human Protein Atlas
OS	Overall survival
DFS	Disease-free survival
HR	Hazard ratio
DMEM	Dulbecco's modified eagle medium
FBS	Fetal bovine serum
PVDF	Polyvinylidene fluoride
BSA	Bovine serum albumin
GO	Gene Ontology
KEGG	Kyoto Encyclopedia of Genes and Genomes
GSEA	Gene set enrichment analysis
FDR	False discovery rate
RLU	Relative light unit
EGF	Epidermal growth factor
AREG	Amphiregulin

Declarations

Ethics approval and consent to participate

All of the experiments were conducted following approval from the Ethics Committees of Peking University. Written informed consent was obtained from all patients prior to tissue sample collection.

Consent for publication

All authors have agreed to publish this manuscript.

Availability of data and materials

All data generated or analyzed during this study are included in this published article.

Competing interests

The authors have no potential conflicts of interest.

Funding

Supported by the National Natural Science Foundation of China (Grant No. 81773765, 81270049, 81874318, 82073878, 61873027), Applied Basic Research Program of Shanxi Province (Grant No. 201901D211470). Project of Development Center for Medical Science and Technology, National Health Commission of the PRC, W2017ZWS17.

Author Contributions

HQY did the experiments and wrote the primary manuscript. DW, ZQW, MN, MYH and JJC gave suggestion and revised the manuscript. HCX did the bioinformatics analysis. PR, SWM, CTL provided clinic cancer patients sample. DMA guided the analysis of data. XJL provided insights. ZQL, SHM and YP planned and guided the experiments and revised the manuscript.

References

1. Bray, F.; Ferlay, J.; Soerjomataram, I.; Siegel, R. L.; Torre, L. A.; Jemal, A., Global cancer statistics 2018: GLOBOCAN estimates of incidence and mortality worldwide for 36 cancers in 185 countries. *CA-Cancer J. Clin.* **2018,** *68* (6), 394-424.
2. Molina, J. R.; Yang, P.; Cassivi, S. D.; Schild, S. E.; Adjei, A. A., Non-small cell lung cancer: epidemiology, risk factors, treatment, and survivorship. *Mayo Clin Proc* **2008,** *83* (5), 584-94.
3. Sung, H.; Ferlay, J.; Siegel, R. L.; Laversanne, M.; Soerjomataram, I.; Jemal, A.; Bray, F., Global Cancer Statistics 2020: GLOBOCAN Estimates of Incidence and Mortality Worldwide for 36 Cancers in 185 Countries. *CA Cancer J Clin* **2021,** *71* (3), 209-249.
4. Collins, L. G.; Haines, C.; Perkel, R.; Enck, R. E., Lung cancer: diagnosis and management. *Am Fam Physician* **2007,** *75* (1), 56-63.
5. Hirsch, F. R.; Scagliotti, G. V.; Mulshine, J. L.; Kwon, R.; Curran, W. J., Jr.; Wu, Y. L.; Paz-Ares, L., Lung cancer: current therapies and new targeted treatments.

Lancet **2017,** *389* (10066), 299-311.
6. Maemondo, M.; Inoue, A.; Kobayashi, K.; Sugawara, S.; Oizumi, S.; Isobe, H.; Gemma, A.; Harada, M.; Yoshizawa, H.; Kinoshita, I.; Fujita, Y.; Okinaga, S.; Hirano, H.; Yoshimori, K.; Harada, T.; Ogura, T.; Ando, M.; Miyazawa, H.; Tanaka, T.; Saijo, Y.; Hagiwara, K.; Morita, S.; Nukiwa, T.; Grp, N. E. J. S., Gefitinib or Chemotherapy for Non-Small-Cell Lung Cancer with Mutated EGFR. *N. Engl. J. Med.* **2010,** *362* (25), 2380-2388.
7. Rosell, R.; Carcereny, E.; Gervais, R.; Vergnenegre, A.; Massuti, B.; Felip, E.; Palmero, R.; Garcia-Gomez, R.; Pallares, C.; Sanchez, J. M.; Porta, R.; Cobo, M.; Garrido, P.; Longo, F.; Moran, T.; Insa, A.; De Marinis, F.; Corre, R.; Bover, I.; Illiano, A.; Dansin, E.; de Castro, J.; Milella, M.; Reguart, N.; Altavilla, G.; Jimenez, U.; Provencio, M.; Moreno, M. A.; Terrasa, J.; Munoz-Langa, J.; Valdivia, J.; Isla, D.; Domine, M.; Molinier, O.; Mazieres, J.; Baize, N.; Garcia-Campelo, R.; Robinet, G.; Rodriguez-Abreu, D.; Lopez-Vivanco, G.; Gebbia, V.; Ferrera-Delgado, L.; Bombaron, P.; Bernabe, R.; Bearz, A.; Artal, A.; Cortesi, E.; Rolfo, C.; Sanchez-Ronco, M.; Drozdowskyj, A.; Queralt, C.; de Aguirre, I.; Ramirez, J. L.; Sanchez, J. J.; Molina, M. A.; Taron, M.; Paz-Ares, L.; Grp Francais, P.; Assoc Italiana Oncologia, T., Erlotinib versus standard chemotherapy as first-line treatment for European patients with advanced EGFR mutation-positive non-small-cell lung cancer (EURTAC): a multicentre, open-label, randomised phase 3 trial. *Lancet Oncol.* **2012,** *13* (3), 239-246.
8. Wu, Y. L.; Zhou, C. C.; Hu, C. P.; Feng, J. F.; Lu, S.; Huang, Y. C.; Li, W.; Hou, M.; Shi, J. H.; Lee, K. Y.; Xu, C. R.; Massey, D.; Kim, M.; Shi, Y.; Geater, S. L., Afatinib versus cisplatin plus gemcitabine for first-line treatment of Asian patients with advanced non-small-cell lung cancer harbouring EGFR mutations (LUX-Lung 6): an open-label, randomised phase 3 trial. *Lancet Oncol.* **2014,** *15* (2), 213-222.
9. Angelousi, A.; Kassi, E.; Ansari-Nasiri, N.; Randeva, H.; Kaltsas, G.; Chrousos, G., Clock genes and cancer development in particular in endocrine tissues. *Endocr Relat Cancer* **2019,** *26* (6), R305-r317.
10. Zeng, Z. L.; Luo, H. Y.; Yang, J.; Wu, W. J.; Chen, D. L.; Huang, P.; Xu, R. H., Overexpression of the circadian clock gene Bmal1 increases sensitivity to oxaliplatin in colorectal cancer. *Clin Cancer Res* **2014,** *20* (4), 1042-52.
11. Xuan, W.; Hsu, W. H.; Khan, F.; Dunterman, M.; Pang, L.; Wainwright, D. A.; Ahmed, A. U.; Heimberger, A. B.; Lesniak, M. S.; Chen, P., Circadian Regulator CLOCK Drives Immunosuppression in Glioblastoma. *Cancer Immunol Res* **2022,** *10* (6), 770-784.
12. Liu, H.; Gong, X.; Yang, K., Overexpression of the clock gene Per2 suppresses oral squamous cell carcinoma progression by activating autophagy via the PI3K/AKT/mTOR pathway. *J Cancer* **2020,** *11* (12), 3655-3666.
13. Sangoram, A. M.; Saez, L.; Antoch, M. P.; Gekakis, N.; Staknis, D.; Whiteley, A.; Fruechte, E. M.; Vitaterna, M. H.; Shimomura, K.; King, D. P.; Young, M. W.; Weitz, C. J.; Takahashi, J. S., Mammalian circadian autoregulatory loop: a timeless ortholog and mPer1 interact and negatively regulate CLOCK-BMAL1-induced transcription. *Neuron* **1998,** *21* (5), 1101-13.

14. Gotter, A. L.; Suppa, C.; Emanuel, B. S., Mammalian TIMELESS and Tipin are evolutionarily conserved replication fork-associated factors. *J Mol Biol* **2007,** *366* (1), 36-52.
15. Unsal-Kaçmaz, K.; Chastain, P. D.; Qu, P. P.; Minoo, P.; Cordeiro-Stone, M.; Sancar, A.; Kaufmann, W. K., The human Tim/Tipin complex coordinates an Intra-S checkpoint response to UV that slows replication fork displacement. *Mol Cell Biol* **2007,** *27* (8), 3131-42.
16. Xie, S.; Mortusewicz, O.; Ma, H. T.; Herr, P.; Poon, R. Y.; Helleday, T.; Qian, C., Timeless Interacts with PARP-1 to Promote Homologous Recombination Repair. *Mol Cell* **2015,** *60* (1), 163-76.
17. Reszka, E.; Przybek, M., Circadian Genes in Breast Cancer. *Adv Clin Chem* **2016,** *75*, 53-70.
18. Yoshida, K.; Sato, M.; Hase, T.; Elshazley, M.; Yamashita, R.; Usami, N.; Taniguchi, T.; Yokoi, K.; Nakamura, S.; Kondo, M.; Girard, L.; Minna, J. D.; Hasegawa, Y., TIMELESS is overexpressed in lung cancer and its expression correlates with poor patient survival. *Cancer Sci* **2013,** *104* (2), 171-7.
19. Elgohary, N.; Pellegrino, R.; Neumann, O.; Elzawahry, H. M.; Saber, M. M.; Zeeneldin, A. A.; Geffers, R.; Ehemann, V.; Schemmer, P.; Schirmacher, P.; Longerich, T., Protumorigenic role of Timeless in hepatocellular carcinoma. *Int J Oncol* **2015,** *46* (2), 597-606.
20. Expression of PER, CRY, and TIM genes for the pathological features of colorectal cancer patients [Retraction]. *Onco Targets Ther* **2016,** *9*, 5699.
21. Zhou, J.; Zhang, Y.; Zou, X.; Kuai, L.; Wang, L.; Wang, J.; Shen, F.; Hu, J.; Zhang, X.; Huang, Y.; Chen, Y., Aberrantly Expressed Timeless Regulates Cell Proliferation and Cisplatin Efficacy in Cervical Cancer. *Hum Gene Ther* **2020,** *31* (5-6), 385-395.
22. Xian, H.; Li, Y.; Zou, B.; Chen, Y.; Yin, H.; Li, X.; Pan, Y., Identification of TIMELESS and RORA as key clock molecules of non-small cell lung cancer and the comprehensive analysis. *BMC Cancer* **2022,** *22* (1), 107.
23. Uhlen, M.; Zhang, C.; Lee, S.; Sjöstedt, E.; Fagerberg, L.; Bidkhori, G.; Benfeitas, R.; Arif, M.; Liu, Z.; Edfors, F.; Sanli, K.; von Feilitzen, K.; Oksvold, P.; Lundberg, E.; Hober, S.; Nilsson, P.; Mattsson, J.; Schwenk, J. M.; Brunnström, H.; Glimelius, B.; Sjöblom, T.; Edqvist, P. H.; Djureinovic, D.; Micke, P.; Lindskog, C.; Mardinoglu, A.; Ponten, F., A pathology atlas of the human cancer transcriptome. *Science* **2017,** *357* (6352).
24. Yang, W.; Soares, J.; Greninger, P.; Edelman, E. J.; Lightfoot, H.; Forbes, S.; Bindal, N.; Beare, D.; Smith, J. A.; Thompson, I. R.; Ramaswamy, S.; Futreal, P. A.; Haber, D. A.; Stratton, M. R.; Benes, C.; McDermott, U.; Garnett, M. J., Genomics of Drug Sensitivity in Cancer (GDSC): a resource for therapeutic biomarker discovery in cancer cells. *Nucleic Acids Res* **2013,** *41* (Database issue), D955-61.
25. Zhou, J.; Liu, B.; Li, Z.; Li, Y.; Chen, X.; Ma, Y.; Yan, S.; Yang, X.; Zhong, L.; Wu, N., Proteomic Analyses Identify Differentially Expressed Proteins and Pathways Between Low-Risk and High-Risk Subtypes of Early-Stage Lung Adenocarcinoma and Their Prognostic Impacts. *Mol Cell Proteomics* **2021,** *20*, 100015.

26. Zhang, X.; Gureasko, J.; Shen, K.; Cole, P. A.; Kuriyan, J., An allosteric mechanism for activation of the kinase domain of epidermal growth factor receptor. *Cell* **2006,** *125* (6), 1137-49.
27. Culy, C. R.; Faulds, D., Gefitinib. *Drugs* **2002,** *62* (15), 2237-48; discussion 2249-50.
28. Campbell, L.; Blackhall, F.; Thatcher, N., Gefitinib for the treatment of non-small-cell lung cancer. *Expert Opin Pharmacother* **2010,** *11* (8), 1343-57.
29. Rong, X.; Liang, Y.; Han, Q.; Zhao, Y.; Jiang, G.; Zhang, X.; Lin, X.; Liu, Y.; Zhang, Y.; Han, X.; Zhang, M.; Luo, Y.; Li, P.; Wei, L.; Yan, T.; Wang, E., Molecular Mechanisms of Tyrosine Kinase Inhibitor Resistance Induced by Membranous/Cytoplasmic/Nuclear Translocation of Epidermal Growth Factor Receptor. *J Thorac Oncol* **2019,** *14* (10), 1766-1783.
30. Bazzani, L.; Donnini, S.; Finetti, F.; Christofori, G.; Ziche, M., PGE2/EP3/SRC signaling induces EGFR nuclear translocation and growth through EGFR ligands release in lung adenocarcinoma cells. *Oncotarget* **2017,** *8* (19), 31270-31287.
31. Zhang, S.; Huang, P.; Dai, H.; Li, Q.; Hu, L.; Peng, J.; Jiang, S.; Xu, Y.; Wu, Z.; Nie, H.; Zhang, Z.; Yin, W.; Zhang, X.; Lu, J., TIMELESS regulates sphingolipid metabolism and tumor cell growth through Sp1/ACER2/S1P axis in ER-positive breast cancer. *Cell Death Dis* **2020,** *11* (10), 892.
32. Zheng, X.; Li, W.; Ren, L.; Liu, J.; Pang, X.; Chen, X.; Kang, D.; Wang, J.; Du, G., The sphingosine kinase-1/sphingosine-1-phosphate axis in cancer: Potential target for anticancer therapy. *Pharmacol Ther* **2019,** *195*, 85-99.
33. Desai, N.; Yang, H.; Chandrasekaran, V.; Kazi, R.; Minczuk, M.; Ramakrishnan, V., Elongational stalling activates mitoribosome-associated quality control. *Science* **2020,** *370* (6520), 1105-1110.
34. D'Souza, A. R.; Minczuk, M., Mitochondrial transcription and translation: overview. *Essays Biochem* **2018,** *62* (3), 309-320.
35. Zhang, Y.; Peng, X.; Yang, H.; Zhao, H.; Xia, B.; You, Y., The expression of the circadian gene TIMELESS in non-small-cell lung cancer and its clinical significance. *Int J Clin Exp Pathol* **2020,** *13* (9), 2297-2304.
36. Aran, V.; Omerovic, J., Current Approaches in NSCLC Targeting K-RAS and EGFR. *Int J Mol Sci* **2019,** *20* (22).
37. da Cunha Santos, G.; Shepherd, F. A.; Tsao, M. S., EGFR mutations and lung cancer. *Annu Rev Pathol* **2011,** *6*, 49-69.
38. Sigismund, S.; Avanzato, D.; Lanzetti, L., Emerging functions of the EGFR in cancer. *Mol Oncol* **2018,** *12* (1), 3-20.
39. Pan, J.; Tao, Y. F.; Zhou, Z.; Cao, B. R.; Wu, S. Y.; Zhang, Y. L.; Hu, S. Y.; Zhao, W. L.; Wang, J.; Lou, G. L.; Li, Z.; Feng, X.; Ni, J., An novel role of sphingosine kinase-1 (SPHK1) in the invasion and metastasis of esophageal carcinoma. *J Transl Med* **2011,** *9*, 157.
40. Rosa, R.; Marciano, R.; Malapelle, U.; Formisano, L.; Nappi, L.; D'Amato, C.; D'Amato, V.; Damiano, V.; Marfè, G.; Del Vecchio, S.; Zannetti, A.; Greco, A.; De Stefano, A.; Carlomagno, C.; Veneziani, B. M.; Troncone, G.; De Placido, S.; Bianco, R., Sphingosine kinase 1 overexpression contributes to cetuximab resistance in human

colorectal cancer models. *Clin Cancer Res* **2013,** *19* (1), 138-47.
41. Martin, J. L.; de Silva, H. C.; Lin, M. Z.; Scott, C. D.; Baxter, R. C., Inhibition of insulin-like growth factor-binding protein-3 signaling through sphingosine kinase-1 sensitizes triple-negative breast cancer cells to EGF receptor blockade. *Mol Cancer Ther* **2014,** *13* (2), 316-28.
42. Wang, X.; Maruvada, R.; Morris, A. J.; Liu, J. O.; Wolfgang, M. J.; Baek, D. J.; Bittman, R.; Kim, K. S., Sphingosine 1-Phosphate Activation of EGFR As a Novel Target for Meningitic Escherichia coli Penetration of the Blood-Brain Barrier. *PLoS Pathog* **2016,** *12* (10), e1005926.
43. Shida, D.; Kitayama, J.; Yamaguchi, H.; Yamashita, H.; Mori, K.; Watanabe, T.; Yatomi, Y.; Nagawa, H., Sphingosine 1-phosphate transactivates c-Met as well as epidermal growth factor receptor (EGFR) in human gastric cancer cells. *FEBS Lett* **2004,** *577* (3), 333-8.
44. Hsu, A.; Zhang, W.; Lee, J. F.; An, J.; Ekambaram, P.; Liu, J.; Honn, K. V.; Klinge, C. M.; Lee, M. J., Sphingosine-1-phosphate receptor-3 signaling up-regulates epidermal growth factor receptor and enhances epidermal growth factor receptor-mediated carcinogenic activities in cultured lung adenocarcinoma cells. *Int J Oncol* **2012,** *40* (5), 1619-26.
45. Ma, Y.; Xing, X.; Kong, R.; Cheng, C.; Li, S.; Yang, X.; Li, S.; Zhao, F.; Sun, L.; Cao, G., SphK1 promotes development of non-small cell lung cancer through activation of STAT3. *Int J Mol Med* **2021,** *47* (1), 374-386.
46. Tamashiro, P. M.; Furuya, H.; Shimizu, Y.; Kawamori, T., Sphingosine kinase 1 mediates head & neck squamous cell carcinoma invasion through sphingosine 1-phosphate receptor 1. *Cancer Cell Int* **2014,** *14* (1), 76.
47. Jin, Z.; Li, H.; Hong, X.; Ying, G.; Lu, X.; Zhuang, L.; Wu, S., TRIM14 promotes colorectal cancer cell migration and invasion through the SPHK1/STAT3 pathway. *Cancer Cell Int* **2018,** *18*, 202.
48. Qin, Z.; Tong, H.; Li, T.; Cao, H.; Zhu, J.; Yin, S.; He, W., SPHK1 contributes to cisplatin resistance in bladder cancer cells via the NONO/STAT3 axis. *Int J Mol Med* **2021,** *48* (5).
49. Rohini, M.; Haritha Menon, A.; Selvamurugan, N., Role of activating transcription factor 3 and its interacting proteins under physiological and pathological conditions. *Int J Biol Macromol* **2018,** *120* (Pt A), 310-317.
50. Li, X.; Zhou, X.; Li, Y.; Zu, L.; Pan, H.; Liu, B.; Shen, W.; Fan, Y.; Zhou, Q., Activating transcription factor 3 promotes malignance of lung cancer cells in vitro. *Thorac Cancer* **2017,** *8* (3), 181-191.
51. Hao, Z. F.; Ao, J. H.; Zhang, J.; Su, Y. M.; Yang, R. Y., ATF3 activates Stat3 phosphorylation through inhibition of p53 expression in skin cancer cells. *Asian Pac J Cancer Prev* **2013,** *14* (12), 7439-44.
52. Hart, P. C.; Chiyoda, T.; Liu, X.; Weigert, M.; Curtis, M.; Chiang, C. Y.; Loth, R.; Lastra, R.; McGregor, S. M.; Locasale, J. W.; Lengyel, E.; Romero, I. L., SPHK1 Is a Novel Target of Metformin in Ovarian Cancer. *Mol Cancer Res* **2019,** *17* (4), 870-881.
53. Pan, Y.; Liu, L.; Zhang, Q.; Shi, W.; Feng, W.; Wang, J.; Wang, Q.; Li, S.; Li, M.,

Activation of AMPK suppresses S1P-induced airway smooth muscle cells proliferation and its potential mechanisms. *Mol Immunol* **2020,** *128*, 106-115.

Figure legends

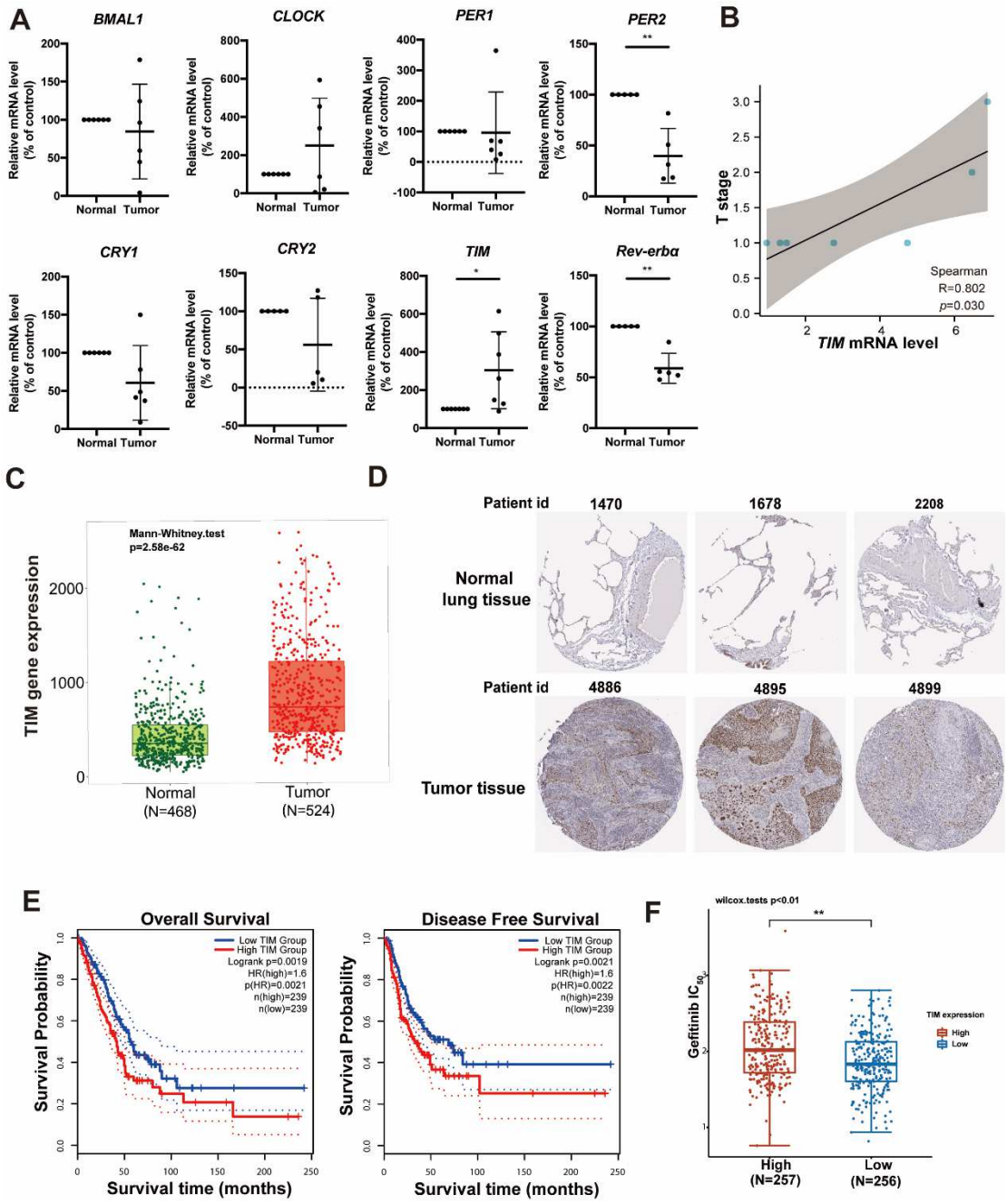

Figure 1. Analysis of TIMELESS (TIM) in lung adenocarcinoma (LUAD), and correlation analysis with patient prognosis. (A) mRNA levels of eight circadian clock genes in the tumor tissues of patients with non-small cell lung carcinoma (NSCLC) and TIM mRNA in LUAD detected by RT-qPCR assay, n = 5–7. (B) Correlation analysis of TIM with pathological stage. Spearman's correlation coefficient is R = 0.802, p = 0.030. (C) Data from the TNMplot database were used to further evaluate the level of TIM in LUAD. The *p*-value test method is shown on the upper left

corner of the figure, and Mann–Whitney test was used for statistical analysis. (D) Immunohistochemical staining images of TIM protein in patients with NSCLC from the HPA database. The upper three images are of normal lung tissues. The lower three images are from NSCLC lung carcinoma tissues. (E) Correlation between the TIM level and overall or disease-free survival of patients with LUAD using data from the GEPIA2 database. The grouping threshold for TIM was set to "Median." Log-rank test was used to compare the survival distributions of two samples. Cox proportional hazard ratios (HRs) are shown in the image. (F) Gefitinib IC_{50} value prediction in patients with LUAD with different TIM levels using the GDSC database. The horizontal axis represents different TIM-level groups, and the vertical axis represents the predicted IC_{50} value of gefitinib. The grouping threshold was set to "Median." Wilcox test was used to conduct statistical analysis.

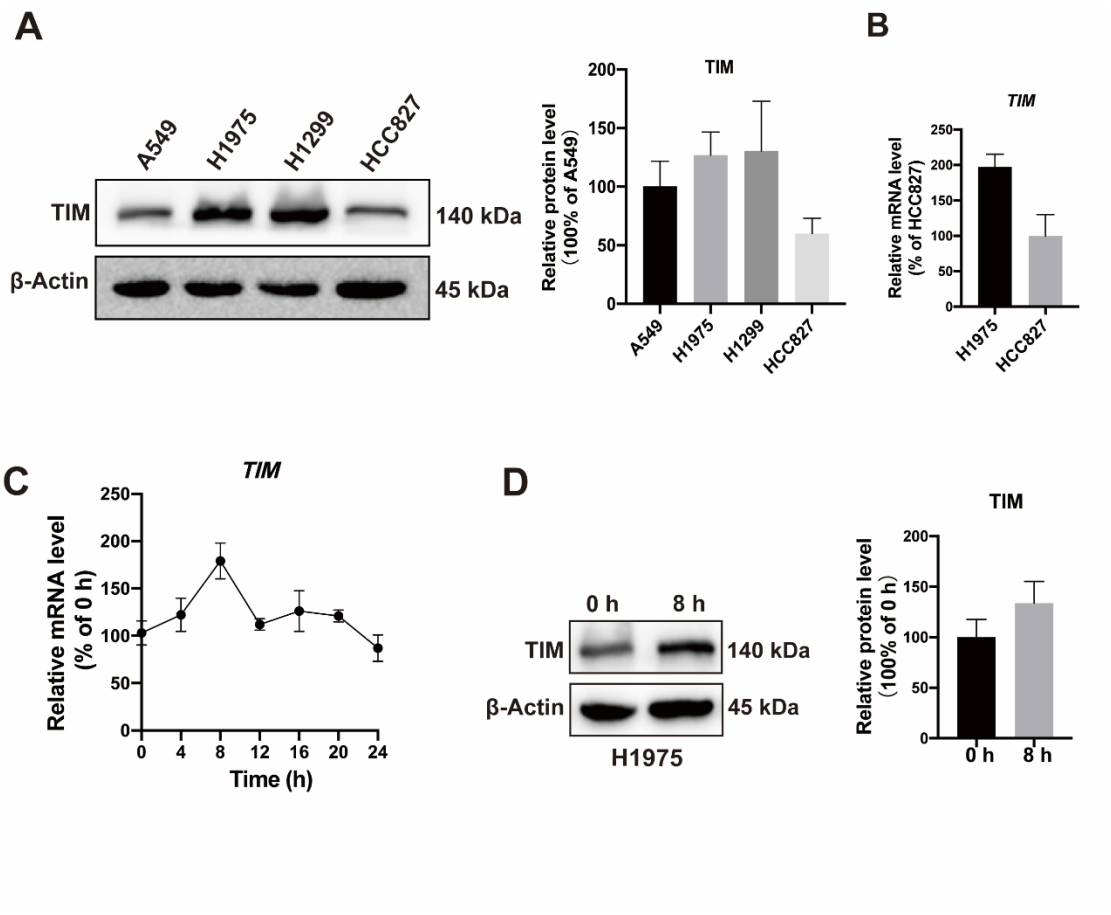

Figure 2. TIM protein expression level and the 24-h dynamic changes in TIM mRNA level in LUAD cells. (A) TIM protein expression levels in A549, H1975, H1299, and HCC827 cells were detected by western blot. (B) *TIM* mRNA levels in H1975 and HCC827 cells were detected by RT-qPCR assay. (C) Dynamic changes of *TIM* mRNA level in H1975 cells within 24 h were detected by RT-qPCR assay. (D) TIM protein expression levels in H1975 cells at 0 h and 8 h were detected by western blot. The grayscale values of the protein bands were analyzed by ImageJ software. Data are shown as the mean ± standard deviation, n = 3–7. The experiments were repeated three times independently.

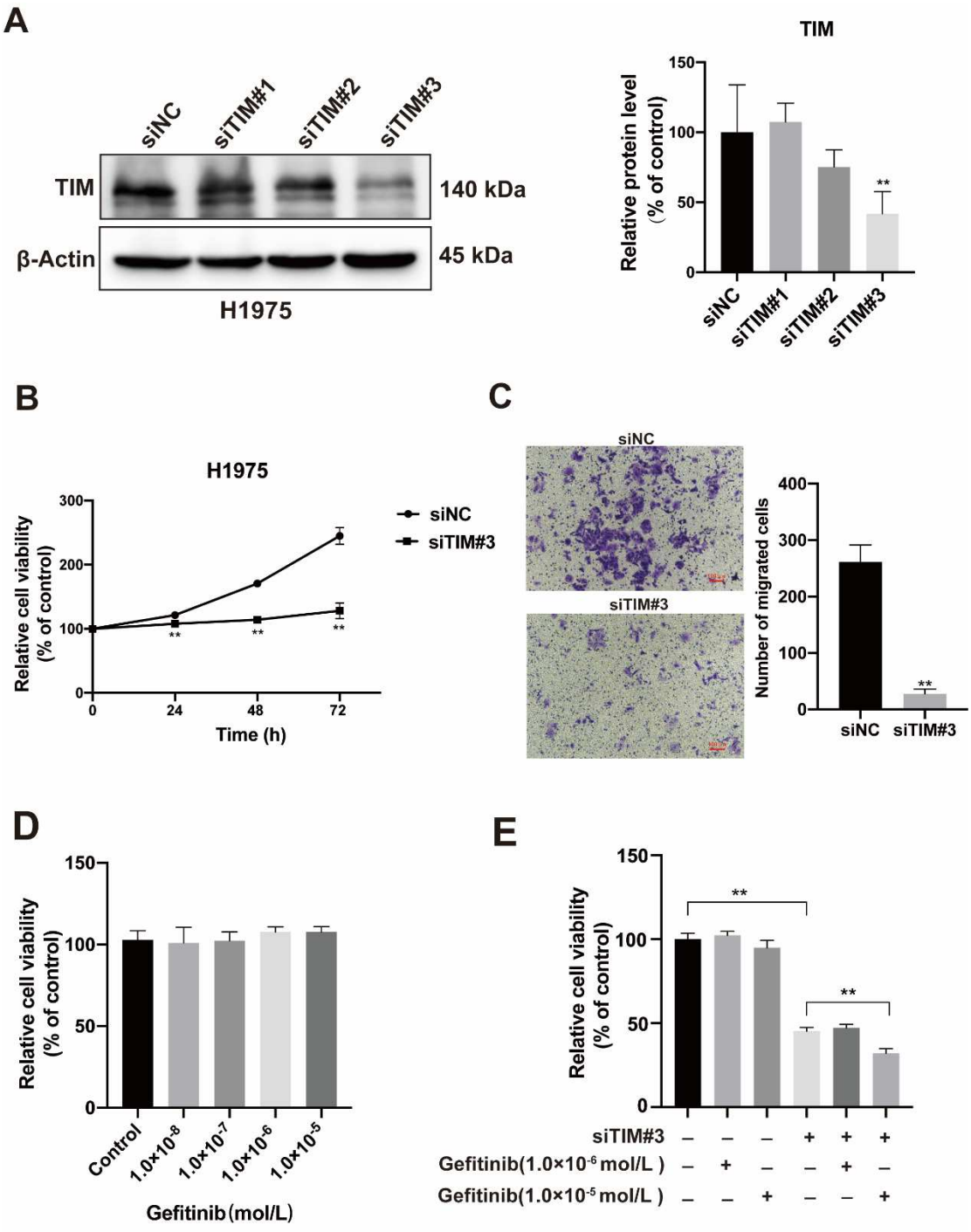

Figure 3. TIM knockdown inhibited the proliferation and migration of LUAD cells and sensitized the antitumor effect of gefitinib. (A) Knockdown efficiency of TIM siRNA in H1975 cells was detected by western blot assay, and the grayscale values of the protein bands were analyzed using Image J software. siNC is the vector control group, siTIM#1 is the first pair TIM siRNA knockdown group, siTIM#2 is the second pair TIM siRNA knockdown group, and siTIM#3 is the third pair TIM siRNA knockdown group. siTIM#3 achieved 53% knock down of TIM expression.

(B) TIM knockdown inhibited the H1975 cell proliferation from 24 h to 72 h, as detected using CCK8 assay. (C) TIM knockdown inhibited H1975 cell migration, as detected with an 8-μm Transwell chamber. Cells that migrated to the backside of Transwell inserts were taken and calculated. Scale bar: 100 μm. (D) Effect of gefitinib on H1975 cell proliferation, as detected using the CCK8 method. (E) TIM knockdown with siTIM#3 improved the anti-proliferation of 10^{-5} M gefitinib in H1975 cells, as detected using the CCK8 method. Data are shown as the mean ± standard deviation, n = 3–5. Student's *t*-test or one-way ANOVA was used for statistical analysis, $^{**}p < 0.01$, compared to the control group. The experiments were repeated three times independently.

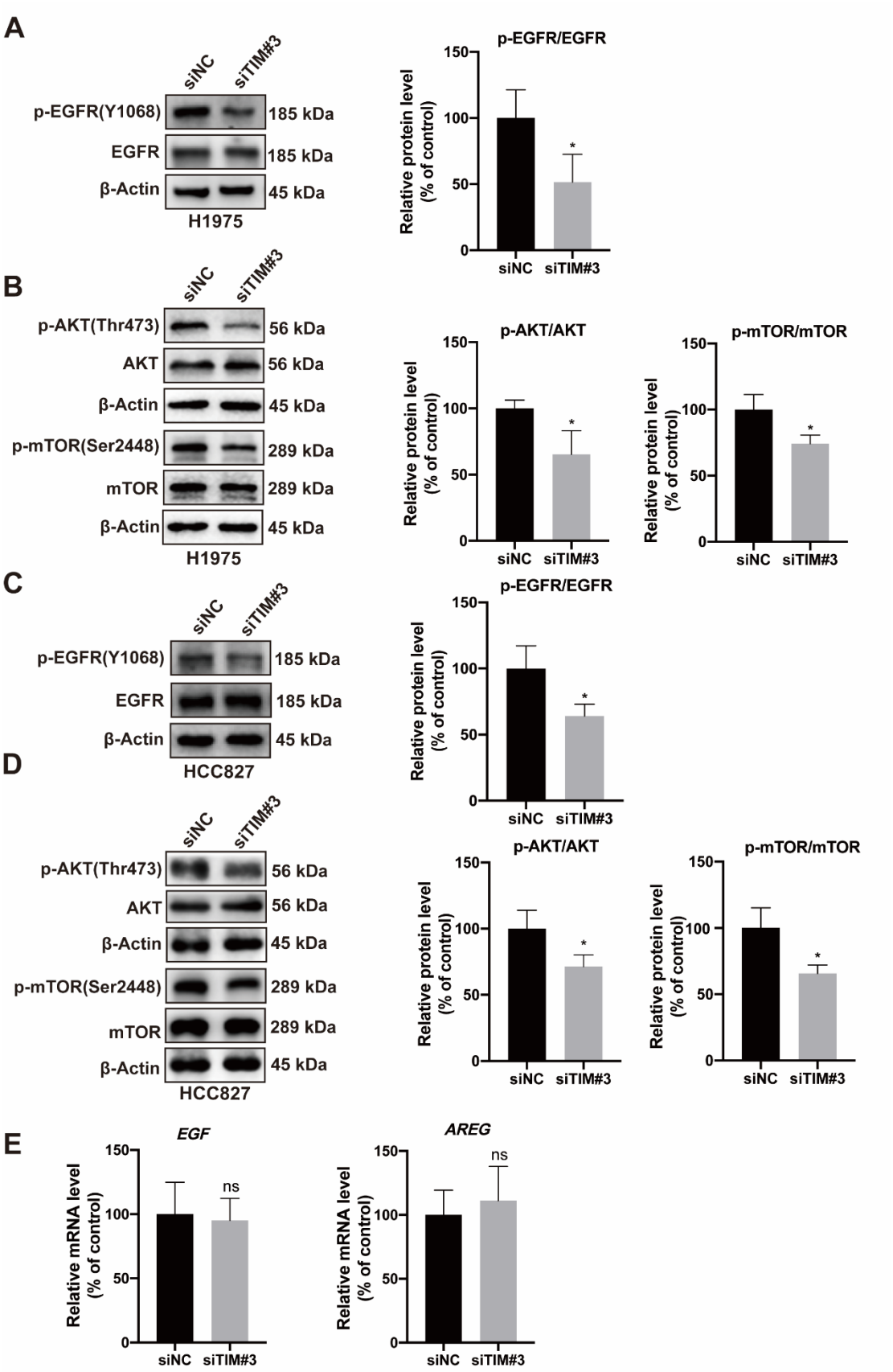

Figure 4. TIM knockdown inhibited EGFR activation and the downstream AKT/mTOR pathway in LUAD cells. (A) Influence of TIM knockdown with siTIM#3 on EGFR activation in

H1975 cells. The EGFR protein expression and EGFR phosphorylation level were detected by western blot. (B) Influence of TIM knockdown with siTIM#3 on AKT/mTOR activation in H1975 cells. (C) Knockdown of TIM with siTIM#3 showed similar inhibitory effects on EGFR activation in HCC827 cells. (D) Knockdown of TIM with siTIM#3 inhibited AKT/mTOR activation in HCC827 cells. (E) Knockdown of TIM expression with siTIM#3 did not affect *EGF* and *AREG* mRNA levels in H1975 cells, as detected by RT-qPCR assay. siNC is the vector control group, and siTIM#3 is the TIM knockdown group. Data are shown as the mean ± standard deviation, n = 3. Student's *t*-test was used for statistical analysis, * $p < 0.05$, compared to the siNC group; ns: no significance. The experiments were repeated three times independently.

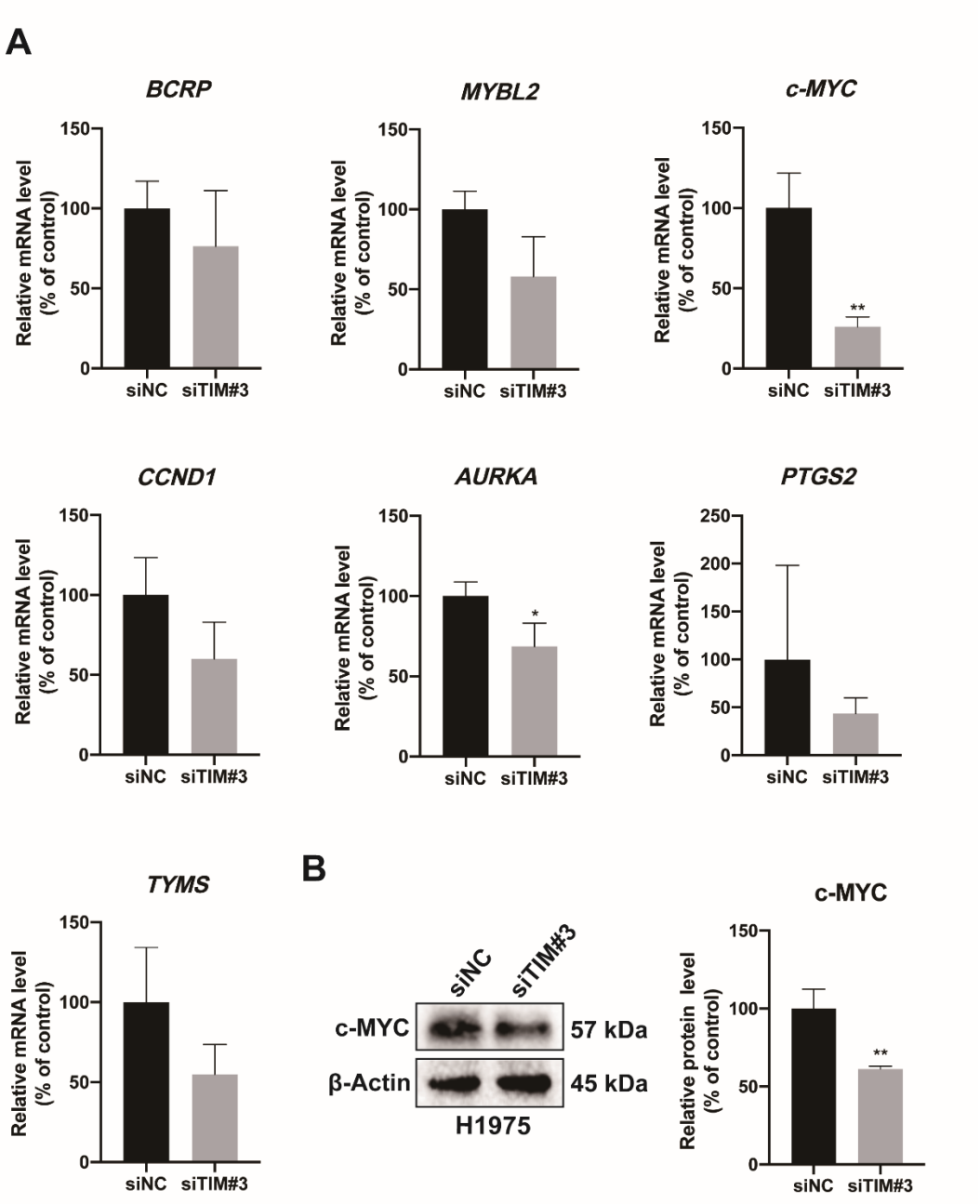

Figure 5. TIM knockdown downregulated the levels of the oncogenes *c-MYC* and *AURKA* in LUAD cells. (A) Changes in the mRNA expression levels of the oncogenes *BCRP*, *MYBL2*, *CCND1*, *c-MYC*, *AURKA*, *PTGS2*, and *TYMS* in H1975 cells following TIM knockdown were detected using RT-qPCR assay. (B) Changes in c-MYC protein expression in H1975 cells caused by TIM knockdown with siTIM#3 were detected by western blot, and the grayscale values of the protein bands were analyzed with ImageJ software. siNC is the vector control group, and siTIM#3 is the knockdown TIM group. Data are shown as the mean ± standard deviation, n = 3. Student's *t*-test

was used for statistical analysis, *$p < 0.05$, **$p < 0.01$, compared to the siNC group. The experiments were repeated three times independently.

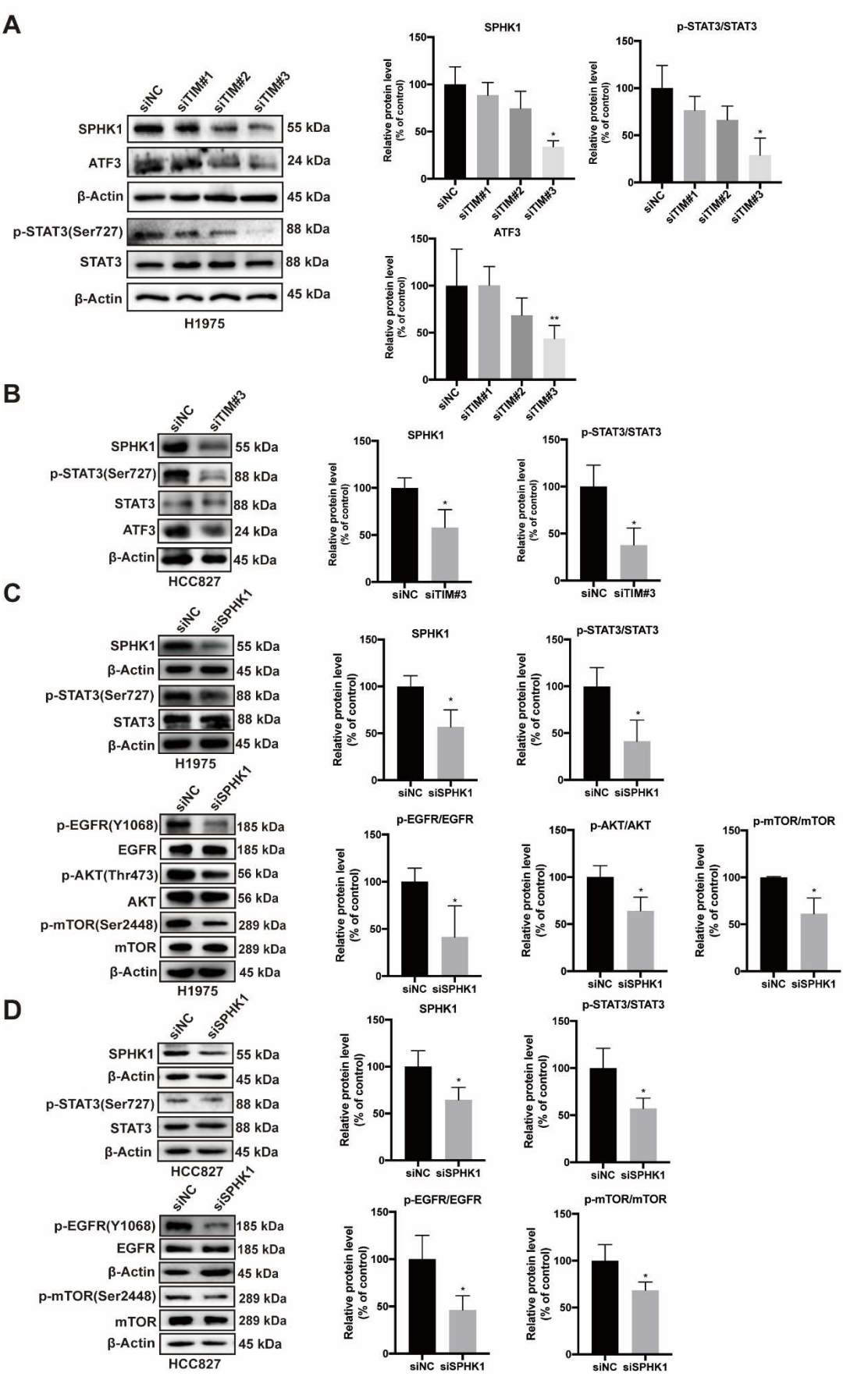
A
siNC
siTIM#1
siTIM#2
siTIM#3
SPHK1
55 kDa
ATF3
24 kDa
β-Actin
45 kDa
p-STAT3(Ser727)
88 kDa
STAT3
88 kDa
β-Actin
45 kDa
H1975
SPHK1
p-STAT3/STAT3
ATF3
Relative protein level (% of control)
B
siNC
siTIM#3
SPHK1
55 kDa
p-STAT3(Ser727)
88 kDa
STAT3
88 kDa
ATF3
24 kDa
β-Actin
45 kDa
HCC827
C
siNC
siSPHK1
SPHK1
55 kDa
β-Actin
45 kDa
p-STAT3(Ser727)
88 kDa
STAT3
88 kDa
β-Actin
45 kDa
H1975
p-EGFR(Y1068)
185 kDa
EGFR
185 kDa
p-AKT(Thr473)
56 kDa
AKT
56 kDa
p-mTOR(Ser2448)
289 kDa
mTOR
289 kDa
β-Actin
45 kDa
H1975
p-EGFR/EGFR
p-AKT/AKT
p-mTOR/mTOR
D
siNC
siSPHK1
SPHK1
55 kDa
β-Actin
45 kDa
p-STAT3(Ser727)
88 kDa
STAT3
88 kDa
β-Actin
45 kDa
HCC827
p-EGFR(Y1068)
185 kDa
EGFR
185 kDa
β-Actin
45 kDa
p-mTOR(Ser2448)
289 kDa
mTOR
289 kDa
β-Actin
45 kDa
HCC827
p-EGFR/EGFR
p-mTOR/mTOR

Figure 6. Regulation of SPHK1 by TIM regulated EGFR activation in LUAD cell lines. Knockdown of TIM with siTIM#3 inhibited SPHK1 expression, STAT3 activation, and ATF3 expression in H1975 (A) and HCC827 cells (B), as detected by western blot. (C) Knockdown efficiency of SPHK1 siRNA in H1975 cells was detected by western blot, which showed significant decreases in STAT3 activation and ATF expression. SPHK1 knockdown also inhibited EGFR and AKT/mTOR activation in H1975 cells (C). siNC is the vector control group, siTIM#1 is the first pair TIM siRNA knockdown group, siTIM#2 is the second pair TIM siRNA knockdown group, and siTIM#3 pair is the third TIM siRNA knockdown group. siSPHK1 is the SPHK1 siRNA knockdown group. Data are shown as the mean ± standard deviation, n = 3. Student's *t*-test or one-way ANOVA was used for statistical analysis, $*p < 0.05$; $**p < 0.01$, compared to the siNC group. The experiments were repeated three times independently.

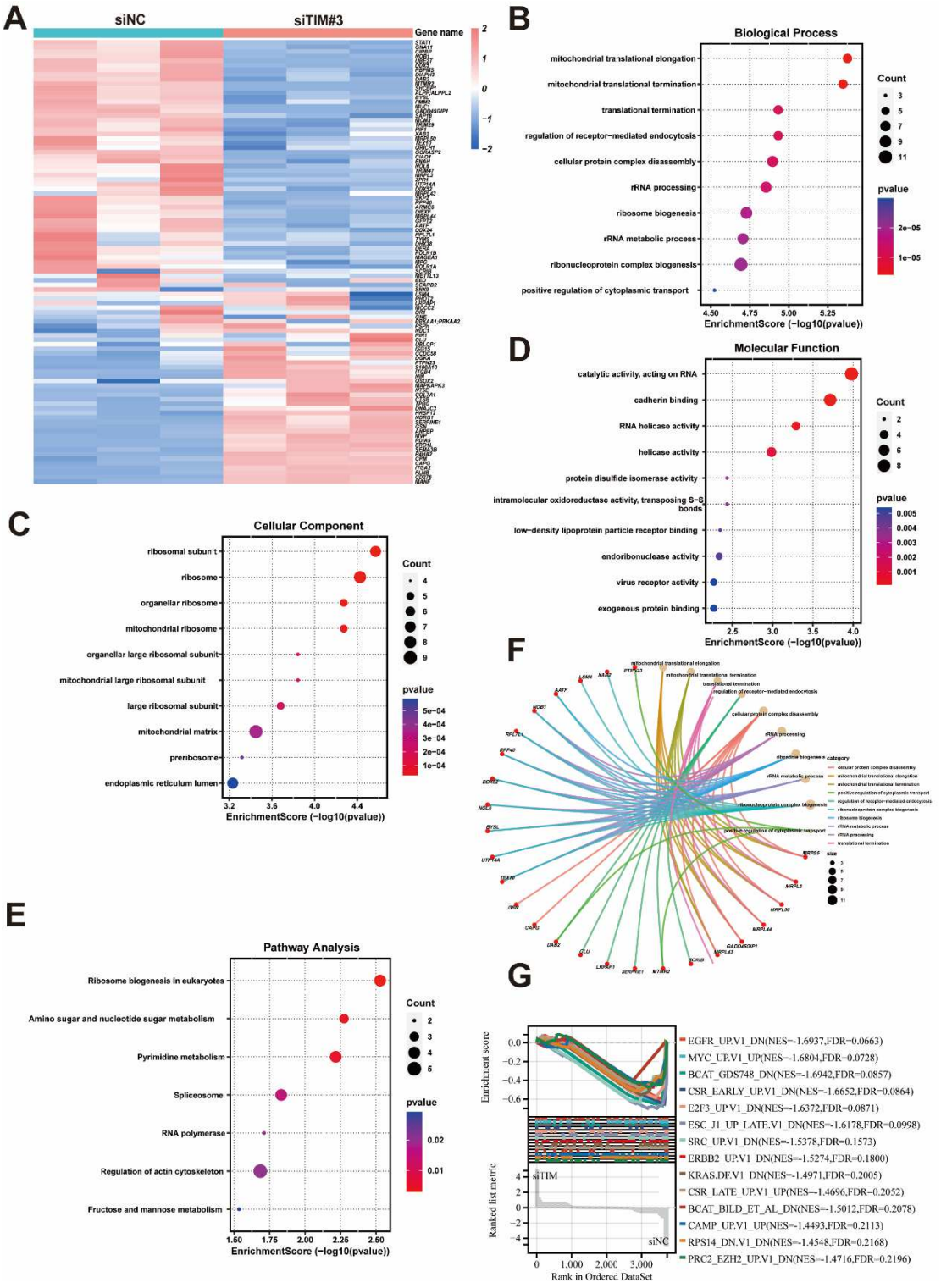

Figure 7. Proteomics combined with bioinformatics analysis of H1975 cells with TIM knockdown. (A) Heatmap of differentially expressed proteins (DEPs) obtained from proteomic analysis between siNC and siTIM treatments. Shades of color indicate relative protein expression levels (red indicates higher expression, blue indicates lower expression level compared to each

other). DEPs were screened according to $|\log_2(FC)| > 1$, adjusted *p-value* < 0.05; n = 3. The gene names corresponding to the protein are shown on the right side of the heatmap. siNC is the vector control group, and siTIM#3 is the TIM knockdown group. Gene Ontology (GO) and Kyoto Encyclopedia of Genes and Genomes (KEGG) pathway enrichment analyses were performed using the R packages "clusterProfiler" and "pathview." (B) GO biological process enrichment analysis. (C) GO cellular component enrichment analysis. (D) GO molecular function enrichment analysis. (E) KEGG pathway enrichment analysis. The size of the dot (count) indicates the number of enriched proteins, and the color (from purple to red) indicates the *p*-value (from large to small accordingly). (F) Proteins involved in the regulation of the first 10 GO biological processes. Brown dots indicate biological processes, red dots indicate proteins (shown here with their gene name), the size of the dots (size) indicates the number of proteins enriched in each biological process, and the lines indicate the association of proteins with biological processes. Different colors are used for different biological processes, with a single color used for each process. (G) Gene set enrichment analysis (GSEA). c6.all.v7.4.symbols.gmt from the Molecular Signatures Database Subsets was used to evaluate related pathways. The minimum gene number was set to 5, and the maximum gene number was set to 5000. NES: normalized enrichment score, FDR: false discovery rate.

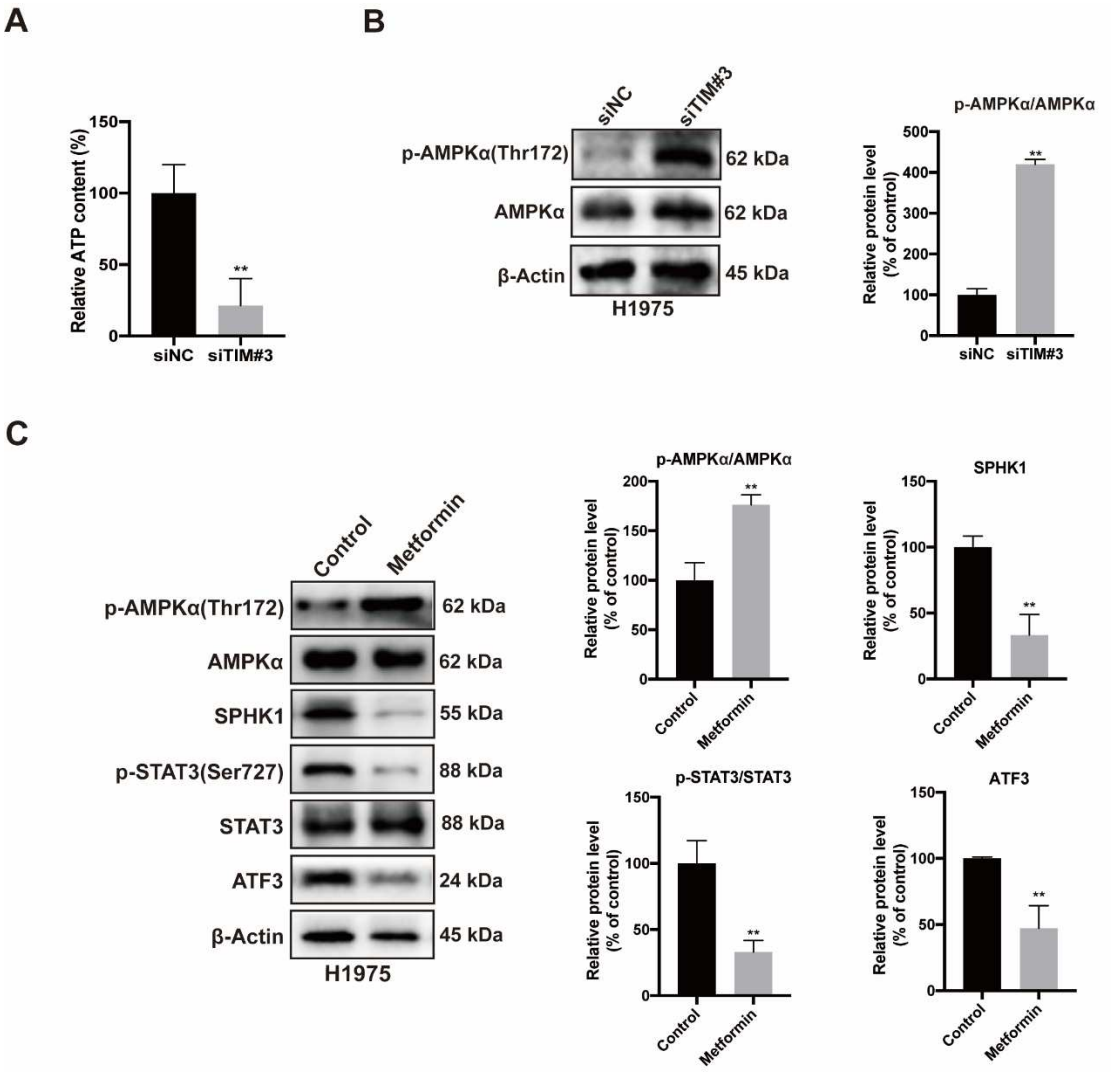

Figure 8. Effect of TIM on mitochondrial function in LUAD cells. (A) TIM knockdown reduced the ATP content in H1975 cells. (B) Knockdown of TIM promoted AMPK activation in H1975 cells, as detected by western blot. (C) Treatment with 10 mmol/L metformin promoted AMPK activation and inhibited SPHK1 expression, STAT3 activation, and ATF3 expression in H1975 cells, as detected by western blot. siNC is the vector control group, and siTIM#3 is the TIM knockdown group. The results are shown as the mean ± standard deviation, n = 3. Student's *t*-test or one-way ANOVA was used for statistical analysis, *$p < 0.05$; **$p < 0.01$, compared to the siNC group. The experiments were repeated three times independently.

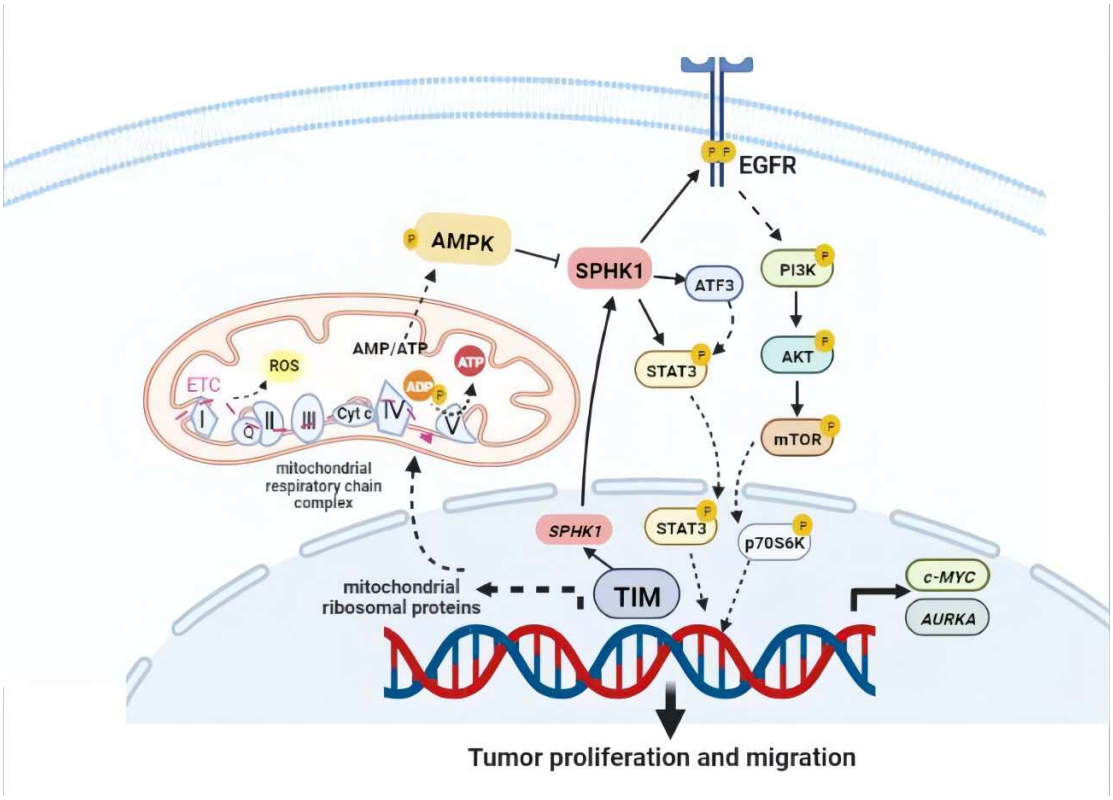

Figure 9. TIM has an important role in NSCLC cell proliferation and migration by influencing the activation of AMPK and SPHK1 and regulating EGFR activation. TIM may have effects on mitochondrial ribosomal proteins and influence mitochondrial ATP content and, subsequently, AMPK activation.

Tables

Table 1. siRNA sequences

Gene	Sense (5′-3′)	Antisense (5′-3′)
Negative control	UUCUCCGAACGUGUCACGUTT	ACGUGACACGUUCGGAGAATT
TIM siRNA#1	GCUAGAGAUUGUCUCCCUUTT	AAGGGAGACAAUCUCUAGCTT
TIM siRNA#2	GCAACAGGCAUUCUCGAUUTT	AAUCGAGAAUGCCUGUUGCTT
TIM siRNA#3	CCAAAUACAUCCUGGGCAATT	UUGCCCAGGAUGUAUUUGGTT
SPHK1 siRNA	GUGCACCCAAACUACUUCUTT	AGAAGUAGUUUGGGUGCACTT

Table 2. RT-qPCR primer sequences

Gene name	Primer sequence (5′-3′)

TIM	Forward primer	GAGACTTCTGCTCTGAGTTCC
	Reverse primer	CCAAGGCCCACATATAATAGGT
BCRP	Forward primer	CAGGTGGAGGCAAATCTTCGT
	Reverse primer	CCCTGTTAATCCGTTCGTTTT
B-Myb	Forward primer	CGGAGCAGAGGGATAGCA
	Reverse primer	CAGTGCGGTTAGGGAAGTGG
CCND1	Forward primer	GCTGCGAAGTGGAAACCATC
	Reverse primer	CCTCCTTCTGCACACATTTGAA
c-MYC	Forward primer	GGCTCCTGGCAAAAGGTCA
	Reverse primer	CTGCGTAGTTGTGCTGATGT
AURKA	Forward primer	GCAGATTTTGGGTGGTCAGT
	Reverse primer	TAGTCCAGGGTGCCACAGA
PTGS2	Forward primer	GCTTTATGCTGAAGCCCTATGA
	Reverse primer	TCCAACTCTGCAGACATTTCC
TYMS	Forward primer	CCCAGTTTATGGCTTCCAGT
	Reverse primer	GCAGTTGGTCAACTCCCTGT
GAPDH	Forward primer	GAGTCCACTGGCGTCTTCAC
	Reverse primer	TGGTTCACACCCATGACGAA
SPHK1	Forward primer	CTGTCACCCATGAACCTGCT
	Reverse primer	TACAGGGAGGTAGGCCAGTC

Table 2. RT-qPCR primer sequences (continued)

Gene name		Primer sequence (5′-3′)
EGF	Forward primer	CATCCATTGGCAAAACCAG
	Reverse primer	AACACCAAGCAGTTCCAAGC
AREG	Forward primer	ATATCACATTGGAGTCACTGCCCA
	Reverse primer	GGGTCCATTGTCTTATGATCCAC
CLOCK	Forward primer	ACGACGAGAACTTGGCATTG
	Reverse primer	TCCGAGAAGAGGCAGAAGG
BMAL1	Forward primer	GGCTGGGGCAGGAAAAATAGG
	Reverse primer	TACTCGTGATGTTCAATGGGC
PER1	Forward primer	CCCAGCACCACTAAGCGTAAA

	Reverse primer	TGCTGACGGCGGATCTTT
PER2	Forward primer	CTTCAGCGATGCCAAGTTTGT
	Reverse primer	CGGATTTCATTCTCGTGGCTTT
CRY1	Forward primer	ACTCCCGTCTGTTTGTGATTCG
	Reverse primer	GCTGCGTCTCGTTCCTTTCC
CRY2	Forward primer	GGTGAAGAACTCAGCAAACGG
	Reverse primer	ACACACATGCTCGCTCTATCTC
REV-ERBα	Forward primer	ATCGTCCGCATCAATCGCAA
	Reverse primer	CTGCTTCTCTCGTTTGGGGAT

Supplementary Figure Legends

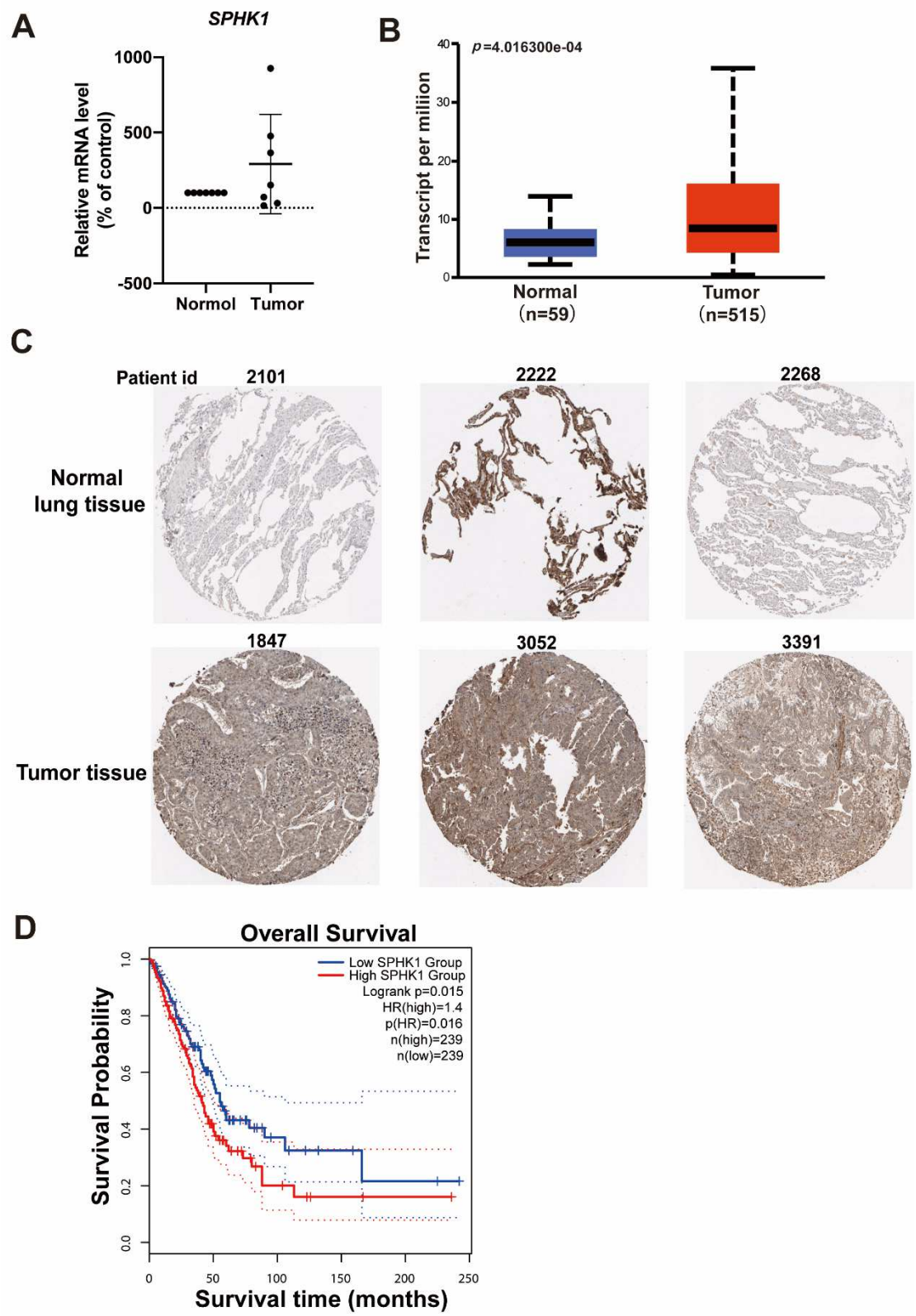

Supplementary Figure 1. SPHK1 is highly expressed in LUAD and correlates with poor

patient prognosis. (A) mRNA level of *SPHK1* in tumor tissues and corresponding para carcinoma tissues of clinic patients with LUAD was detected by RT-qPCR assay. (B) Expression level of SPHK1 in LUAD was reconfirmed using the UALCAN database. The *p*-value is shown in the upper left corner. Compared to normal lung tissues, the expression level of SPHK1 was significantly upregulated in tumor tissues of patients with LUAD ($p < 0.01$). (C) Immunohistochemical staining images of SPHK1 expression in patients with LUAD (ID 1847, 3052, 3391) from the HPA database. The upper image shows the SPHK1 immunohistochemical staining in normal lung tissues, and the lower image shows the SPHK1 immunohistochemical staining in tumor tissues. (D) Expression level of SPHK1 was significantly negatively correlated with the overall survival of patients with LUAD ($p < 0.01$). The grouping threshold for SPHK1 was set to "Median." Log-rank test was used to conduct statistical analysis. Cox proportional hazard ratios (HRs) and 95% confidence intervals are shown in the image.

Supplementary Files

This is a list of supplementary files associated with this preprint. Click to download.

- SupplementalFIG.tif